

Softer Zwitterionic Nanogels for Longer Circulation and Lower Splenic Accumulation

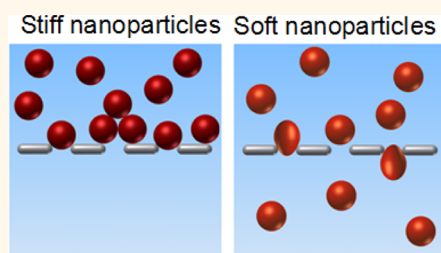
Lei Zhang, Zhiqiang Cao, Yuting Li, Jean-Rene Ella-Menye, Tao Bai, and Shaoyi Jiang*

Department of Chemical Engineering, University of Washington, Seattle, Washington 98195, United States

Long-circulating nanoparticles are highly desirable in drug delivery and diagnosis.^{1,2} Nanoparticles can encapsulate therapeutic drugs and/or imaging reagents, such as magnetic nanoparticles for magnetic resonance imaging (MRI) or quantum dots for fluorescence imaging.^{3,4} They are commonly administered into the body *via* intravenous injection, can stay in the circulation for a desirable long period, and travel with the bloodstream to their targeted site to accumulate in a favorable amount. Long-circulating nanoparticles have two major advantages. They can efficiently stabilize and protect their loadings, which are either unstable in physiological environment or will be quickly degraded in the blood or cleared from the blood circulation. At the same time, they can preferentially deliver their loadings to the targeted site to improve their therapeutic efficiency and/or imaging sensitivity, as well as to reduce accumulation in normal tissues, and thus avoid any potential side effects.^{5,6} Therefore, long-circulating nanoparticles are attracting significant attention and are expected to revolutionize current medical treatments.

To achieve long circulation time *in vivo*, nanoparticles need to be elaborately designed to overcome the intrinsic defense system of the body and the *in vivo* physiological barriers. Several physiological factors are regarded as the important reasons for the clearance of the nanoparticles. First, the blood is a heterogeneous complex medium containing ions, proteins, blood cells, *etc.* It has been well-recognized that immediately after nanoparticles enter the bloodstream, they are susceptible to nonspecific plasma protein adsorption, known as opsonization.⁷ This phenomenon will result in the recognition of the "protein-contaminated" nanoparticles by the reticuloendothelial system (RES), which mainly locates in liver, spleen, and bone marrow,⁸ subsequently leading to the

ABSTRACT



Zwitterionic nanogels of varying stiffness were prepared by tuning their cross-linking densities and reactant contents. *In vivo* studies of these nanogels show that softer nanogels pass through physiological barriers, especially the splenic filtration, more easily than their stiffer counterparts, consequently leading to longer circulation half-life and lower splenic accumulation. Results from this work emphasize the role of stiffness in designing long-circulating nanoparticles.

KEYWORDS: zwitterionic · long-circulating nanoparticles · splenic filtration · nanoparticle stiffness · drug delivery

clearance of the nanoparticles by the RES. Second, nanoparticles in blood circulation are susceptible to splenic filtration. The spleen is the biggest filter of the body. Its unique structure enables the removal of older erythrocytes from the blood circulation as well as blood-borne microorganisms and cellular debris.⁹ The spleen can also filter nanoparticles. It has been reported that the slit size in the spleen rarely exceeds 200 to 500 nm in width, even with an erythrocyte in transit.¹ However, biodistribution studies in the literature show that the spleen has a capability for the filtration of nanoparticles even smaller than 100 nm, and that it can have even higher uptake of nanoparticles per unit mass than liver.^{10–12} Third, although smaller nanoparticles can better avoid splenic filtration, nanoparticles smaller than 20 nm can be excreted by renal clearance in the kidney. The smaller the

* Address correspondence to sjiang@uw.edu.

Received for review March 15, 2012 and accepted July 25, 2012.

Published online July 25, 2012
10.1021/nn301159a

© 2012 American Chemical Society

nanoparticles, the faster the excretion rate.¹³ In addition, some studies also suggested that nanoparticles should be greater than 120 nm to avoid the particles being trapped in the disse and hepatic parenchymal space.¹

By considering all of these factors, nanoparticles should have the following characteristics in order to exhibit long blood circulation. First of all, nanoparticles need to have a stealthy surface coating in order to efficiently stabilize them in complex media and minimize opsonization after they are injected into the bloodstream. Thus, the nanoparticles can evade non-specific uptake by the RES. Furthermore, the nanoparticles need to be designed to bypass several *in vivo* clearance mechanisms, such as the splenic filtration and the renal clearance, to remain in the blood circulation.¹

Current studies of long-circulating nanoparticles are mainly focused on optimizing nanoparticle sizes or coating thicknesses. For example, Perrault *et al.* coated gold nanoparticle cores of five different sizes with polyethylene glycol (PEG) of three different molecular weights and tested circulation time of the PEGylated gold nanoparticles in a mouse model.¹⁰ Results showed that the nanoparticles with the smallest core, but the largest PEG, possessed the longest circulation time. In addition, several studies showed that the nanoparticles' shapes could also influence the circulation time and biodistribution. Nonspherical nanoparticles were found to have longer circulation time than their spherical counterparts.^{14,15}

While the effects of nanoparticle surface coatings, nanoparticle sizes, and shapes have been studied, the mechanical properties of nanoparticles have not been well investigated yet. Mechanical properties play an important role in many biological processes. For example, red blood cells can pass through splenic filtration due to their extraordinary deformability and flexibility. Therefore, they have an *in vivo* longevity of about 120 days. Aged red blood cells finally get cleared from the blood circulation by splenic filtration because they become rigid and have lost these properties.⁹ To prepare artificial red blood cells for biomedical applications, mechanical properties are one important design parameter. Interestingly, DeSimone *et al.* showed the circulation time and biodistribution of micrometer-sized hydrogel disks (about 6 μm in diameter and 2 μm thick) mimicking red blood cells.¹⁶ Several microdisks of varying stiffness were tested. Results showed that softer particles could pass through lung tissue better and possess longer circulation time while their stiffer counterparts were mostly entrapped in lung tissue. In this work, we demonstrate nanosized particles (*i.e.*, nanogels of about 100 nm in diameter) with tunable flexibility, study the relationship between the mechanical and *in vivo* biological properties of engineered nanoparticle, and push the limit of their blood circulation time. Prolonged circulation time can render less

uptake of the nanoparticles by the RES and better chance to arrive the target sites, leading to better efficiency. Long circulation time is fundamentally important for many biomedical applications such as drug delivery and molecular imaging.¹

One efficient method of tuning mechanical properties (*e.g.*, stiffness) of biomaterials is to change their cross-linking density in hydrogels. However, because of the different nature of the monomers and the cross-linkers, this method inevitably induces change in the surface properties of hydrogel as the hydrogel composition varies. Tuning the stiffness of the nanogels without compromising their surface properties still remains a challenge.¹⁷

Here, we present a solution to make stealthy nanogels with tunable "softness" by using zwitterionic monomers and cross-linkers. Zwitterionic materials, such as poly(carboxybetaine) (pCB) and poly(sulfobetaine) (pSB), have been emerging as a new class of materials for constructing long-circulating nanoparticles.¹⁸ They have proved their excellent ultralow fouling properties (<0.3 ng/cm² adsorbed proteins) on flat surfaces¹⁸ or nanoparticle surfaces.¹⁹ It was demonstrated that pCB-coated magnetic nanoparticles (pCB-MNPs) had long-term stability in both saline solutions and 100% human blood serum. These *in vitro* studies revealed pCB-MNPs could efficiently evade the uptake of nonspecific macrophage cells, indicating their weak interactions with the RES.²⁰ However, the *in vivo* environment is far more complicated than any existing *in vitro* models. *In vivo* experiments need to be conducted to evaluate the blood circulation time of pCB nanoparticles. In this work, we prepared stealthy pCB nanogels with different stiffnesses by tuning their cross-linking densities and solid contents. A zwitterionic cross-linker containing a carboxylbetaine group was used to make the nanogels completely zwitterionic without compromising the stealthy properties of the nanogels.²¹

RESULTS AND DISCUSSION

PCB nanogels loaded with gold nanoparticles were prepared by an inverse microemulsion polymerization method.²² To validate our hypothesis *in vitro*, two types of pCB nanogels (one stiff and one soft) were prepared, using 46% reactant content with 15 and 2% cross-linking densities, respectively. The mean hydrodynamic sizes of both the nanogels were tuned to be around 0.25 μm . Syringe filters with cellulose acetate membranes with a pore size of 0.22 μm were used to test the ability of the nanogels to pass through slits narrower than their sizes. The cellulose acetate membrane is hydrophilic and does not adsorb the nanogels on its surface. Both of the nanogel samples show purplish red color due to their encapsulation of gold nanoparticles. The filtration tests are shown in Figure 1. For the "hard" nanogel sample (Figure 1a), the filtrate collected in the cuvette was almost transparent,

indicating most of the hard nanogels were stopped by the filter. Elementary analysis of gold showed that only about 6% of the stiff nanogels were found in the filtrate. In contrast, as shown in Figure 1b, the soft nanogels could efficiently pass through the filter, and the filtrate collected in the cuvette showed similar color as the original sample. Elementary analysis showed that nearly 100% of the soft nanogels remained in the filtrate. The hydrodynamic size of the soft nanogels after filtration was also tested; no change could be observed, indicating the nanogels remained intact during filtration. Scanning electron microscopy (SEM) images (Figure S-1 in the Supporting Information) of the soft nanogels before and after filtration further proved the integrity of the nanogels after filtration. No leakage of gold nanoparticles or breakage of nanogels occurred during the filtration. This result suggests that the soft nanogels are able to pass through narrow slits due to their deformability, as illustrated in Figure 1c,d.

For the *in vivo* tests, five different pCB nanogels with different stiffnesses were prepared using different reactant formations: 46% solid content with 15, 10, 5, and 2% cross-linking densities (denoted as “15%”,

“10%”, “5%”, and “2%”) and 40% solid content with 2% cross-linking density (denoted as “2%-”). Gold nanoparticles are used as a detectable marker and encapsulated in the nanogels, noting that the gold concentration in the blood can be negligible. Thus, the blood concentration of the nanogel samples can be analyzed by an elementary method.

All of the pCB nanogels prepared for *in vivo* tests possess the similar hydrodynamic size of about 120 nm with a polydispersity index (PDI) < 0.1 in phosphate buffered saline (PBS) solution as determined by dynamic light scattering, indicating their uniform size distribution, and their size remains unchanged in PBS solution for at least 60 days, as shown in Figure S-2. These nanoparticles presented a uniform morphology under SEM, as shown in Figure S-3. Macrophage cell uptake tests were conducted to confirm the stealthy properties of all nanogels. When incubated in the medium with macrophage cells, protein adsorption from the cell culture medium onto the surface of nanoparticles can lead to cellular recognition and uptake. As shown in Figure S-4, all nanogel samples, regardless of their cross-linking densities, showed a negligible uptake amount as compared to blank cells and uncoated gold nanoparticles, indicating their strong ability to evade recognition by macrophage cells. While the nanogel samples have similar hydrodynamic size, zeta-potential, gold concentration, and stealthy properties, the only difference is their stiffness, as presented in Table 1; the 2%- sample has the lowest stiffness, while the 15% sample has the highest stiffness.

The *in vivo* circulation results are shown in Figure 2. The circulation half-lives of all samples in rats, ranging from

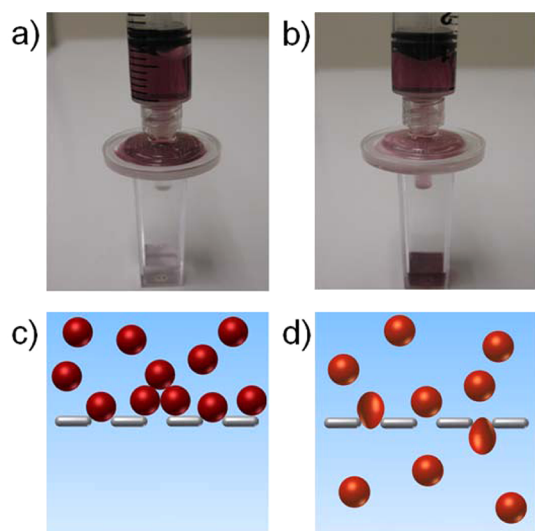


Figure 1. Photo images showing the ability of hard (a) and soft (b) nanogels with a mean hydrodynamic size of $0.25 \mu\text{m}$ to pass filters with a pore size of $0.22 \mu\text{m}$. Schemes showing the interactions of hard particles and soft particles with slits smaller than their size; the hard particles (c) are trapped by the slit, while the soft particles (d) can deform and pass through the slit.

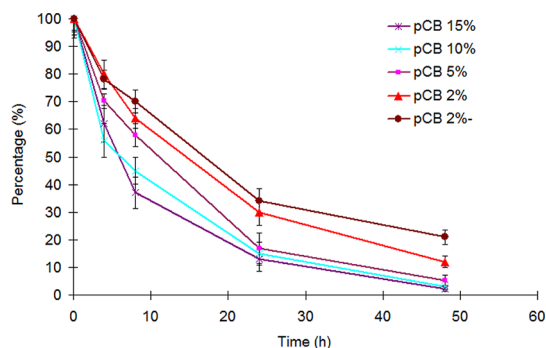


Figure 2. *In vivo* blood circulation profiles of nanogels of varying stiffness encapsulated with gold nanoparticles.

TABLE 1. *In Vitro* and *In Vivo* Characterization of pCB Nanogels

cross-linking density	hydrodynamic size (nm)	PDI	zeta-potential (mv)	gold concentration (%)	modulus of bulk hydrogel (MPa)	<i>in vivo</i> circulation half-life (h)
15%	117.5 ± 4.8	0.07 ± 0.02	-4.5 ± 1.3	11.9 ± 0.3	1.35 ± 0.02	9.1 ± 2.5
10%	120.4 ± 3.4	0.06 ± 0.01	-5.7 ± 2.6	12.2 ± 0.2	0.87 ± 0.03	10.2 ± 1.8
5%	121.8 ± 5.9	0.08 ± 0.02	-3.1 ± 1.5	11.9 ± 0.4	0.58 ± 0.08	11.8 ± 1.7
2%	119.6 ± 3.7	0.06 ± 0.01	-4.8 ± 1.7	12.1 ± 0.3	0.26 ± 0.04	15.0 ± 1.8
2%-	123.3 ± 5.1	0.08 ± 0.01	-3.9 ± 1.3	12.8 ± 0.2	0.18 ± 0.03	19.6 ± 1.5

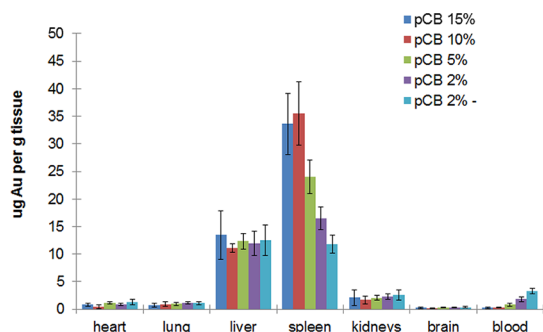


Figure 3. Biodistribution of pCB nanogels with varying stiffness 48 h after injection. Except for between the “10%” and “15%” samples, all samples show a significant decrease ($p < 0.05$) in splenic accumulation as their stiffness decreases.

9.1 to 19.6 h, were calculated using a one-compartment model and are listed in Table 1. Perrault *et al.* reported the circulation studies of several PEG-coated gold nanoparticles with a hydrodynamic size of around 100 nm in a mouse model. These particles possessed *in vivo* circulation half-lives from 3.3 to 11.3 h (also calculated from a one-compartment model), depending on the molecular weights of PEG and the core sizes of gold nanoparticles.¹⁰ Several other long-circulating nanoparticles have circulation half-lives around 10 h.^{12,13,23} Thus, all of the samples in this work can be considered to possess long-circulating properties. It has been reported that uncoated gold nanoparticles are quickly cleared from blood circulation after intravenous injection.^{10,24} Therefore, our results show the strong ability of pCB polymer to protect gold nanoparticles from being cleared. Moreover, it can be clearly observed from the circulation profiles that nanogel samples of varying stiffness have different blood retention half-lives at the same time point. In general, softer nanogels can remain in the bloodstream longer than their stiffer counterparts. As discussed previously, this phenomenon is likely because softer nanogels have better deformability to pass through *in vivo* barriers, especially in the spleen, which is well-known for filtering out rigid particles from the blood circulation.

To further investigate how the nanogels were cleared from the blood circulation, biodistribution studies were performed and the accumulation of nanogel samples in different organs 48 h after administration was tested. As shown in Figure 3, liver and spleen are the major organs responsible for removing nanogels from blood circulation, as reported in the literature,^{10,12,25} since they are the major RES organs clearing foreign blood-borne particulate entities. As expected, other organs show much lower accumulation of the nanogels. Unlike spleen, accumulation of the nanogels in liver as well as other organs shows no significant difference. This is likely due to the fact that all of the nanogel samples have similar surface properties, as shown in the *in vitro* uptake tests of macrophages. Thus, they have similar interactions with

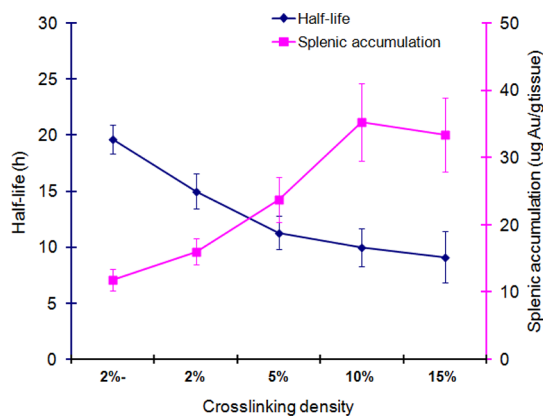


Figure 4. Circulation half-life and splenic accumulation of different nanogel samples.

the RES tissue in liver and other organs. In contrast, accumulation in spleen shows obvious difference among different nanogel samples. The splenic accumulation significantly increases as the nanogels become stiffer, from sample 2%- to sample 10%, while no significant difference can be observed for the 10% and 15% samples. These results show a strong capability for the filtration of nanoparticles by the slits in the walls of venous sinuses in spleen.¹ Consistent with the *in vitro* test, softer nanogels can pass through those slits better and remain in the circulation, while harder nanogels can be retained or trapped and consequently are cleared by the red-pulp macrophages.⁹

To correlate the circulation and biodistribution studies, the circulation half-life was calculated using a one-compartment model and plotted together with the splenic accumulation data. As shown in Figure 4, softer nanogels have longer circulation time but less splenic accumulation. Consistent with our hypothesis, softer nanogels are able to overcome those *in vivo* barriers better, and spleen is the major organ that clears stiffer nanogels.

CONCLUSIONS

In this work, we demonstrate the long-circulating properties of pCB-based nanoparticles using pCB nanogels. Results show that the stiffness of nanoparticles plays an important role in their *in vivo* behaviors. Softer particles are preferred due to their deformability. The findings from this work open new opportunities for the design of long-circulating nanoparticles. It can be a possible solution for some dilemmas in certain applications. For example, when long-circulating drug-loaded nanoparticles are prepared, there is a trade-off between drug loading and circulation half-life. Smaller particles have a longer circulation half-life but less drug loading and easier drug leakage, while larger particles can improve the drug loading and retain drug better but with shorter circulation half-life.^{26,27} In our previous work, we have shown that pCB nanogels have the ability to load and release many types of macromolecular

therapeutic reagents, such as proteins and nucleic acids. On the basis of this work, it can be expected that larger,

but softer, nanogels will achieve high drug loading and extended circulation half-life.²²

METHODS

Preparation of pCB Nanogels. PCB nanogels loaded with gold nanoparticles were prepared by an inverse microemulsion polymerization method.²²

To prepare nanogels for *in vivo* tests, 1.4 g of Tween 80, 2 g of Span 80, and 4 mg of V-70 were dissolved in 20 mL of hexane and kept in an ice bath. Twenty-five milligrams of gold nanoparticles (~10 nm), CBMA, and CB cross-linker were dissolved in 0.35 mL of DI water. The reactant content is 46% for four nanogel samples with cross-linking densities of 2, 5, 10, and 15%. One sample has reactant content of 40% with 2% cross-linking density. The two stock solutions were mixed in a 100 mL flask with vigorous stirring, then strong sonication was applied to form the microemulsion. The flask was purged with nitrogen at 4 °C for 30 min to remove dissolved oxygen. During polymerization, the reaction was kept at 40 °C with stirring and was protected under nitrogen for 12 h. After the reaction, the product was washed by tetrahydrofuran three times to remove the surfactants, then the product was dispersed in DI water and other impurities were removed by using a 100 kDa molecular weight cutoff Amicon Ultra centrifugal filter.

To prepare nanogels for the syringe filtration test, 0.2 g of Tween 80, 0.3 g of Span 80, and 4 mg of V-70 were dissolved in 20 mL of hexane and kept in an ice bath. Twenty-five milligrams of gold nanoparticles (~10 nm), CBMA, and CB cross-linker were dissolved in 0.5 mL of DI water. The reactant content is 46%, and the cross-linking densities are 2 and 15%.

Animal Studies. The *in vivo* circulation time and biodistribution of pCB nanogels are studied using Sprague Dawley rats (body weight 150 g) as the animal model. Each nanogel sample has three duplicates to generate statistical significance. All animal experiments adhered to federal guidelines and were approved by the University of Washington Animal Care and Use Committee. To study the *in vivo* circulation time, 100 μ L of each nanogel sample was administered into the rat *via* tail vein injection at the dose of 1 mg gold per kg body weight. At 5 min, 4 h, 8 h, 24 h, and 48 h after the injection, a 50 μ L blood sample was collected, digested, and analyzed by the elementary analysis method, inductively coupled plasma (ICP). The *in vivo* biodistribution was tested 48 h after the nanogel sample injection. The animals were euthanized by CO₂ inhalation, and the organs (heart, liver, spleen, lung, kidneys, and brain) were collected, lysed in aqua regia, and analyzed by ICP.

Conflict of Interest: The authors declare no competing financial interest.

Acknowledgment. Authors acknowledge support by the Office of Naval Research (N000140910137) and the National Science Foundation (DMR-1005699).

Supporting Information Available: Detailed *in vitro* macrophage uptake, SEM images of soft nanogels before and after filtration by the filter, stability tests in PBS, and SEM image of nanogels for *in vivo* test. This material is available free of charge *via* the Internet at <http://pubs.acs.org>.

REFERENCES AND NOTES

- Moghimi, S. M.; Hunter, A. C.; Murray, J. C. Long-Circulating and Target-Specific Nanoparticles: Theory to Practice. *Pharmacol. Rev.* **2001**, *53*, 283–318.
- Gu, F.; Zhang, L.; Teplý, B. A.; Mann, N.; Wang, A.; Radovic-Moreno, A. F.; Langer, R.; Farokhzad, O. C. Precise Engineering of Targeted Nanoparticles by Using Self-Assembled Biointegrated Block Copolymers. *Proc. Natl. Acad. Sci. U.S.A.* **2008**, *105*, 2586–2591.
- Zhang, L.; Yu, F. Q.; Cole, A. J.; Chertok, B.; David, A. E.; Wang, J. K.; Yang, V. C. Gum Arabic-Coated Magnetic Nanoparticles for Potential Application in Simultaneous Magnetic Targeting and Tumor Imaging. *AAPS J.* **2009**, *11*, 693–699.
- van Schooneveld, M. M.; Vucic, E.; Koole, R.; Zhou, Y.; Stocks, J.; Cormode, D. P.; Tang, C. Y.; Gordon, R. E.; Nicolay, K.; Meijerink, A.; *et al.* Improved Biocompatibility and Pharmacokinetics of Silica Nanoparticles by Means of a Lipid Coating: A Multimodality Investigation. *Nano Lett.* **2008**, *8*, 2517–2525.
- Peer, D.; Karp, J. M.; Hong, S.; Farokhzad, O. C.; Margalit, R.; Langer, R. Nanocarriers as an Emerging Platform for Cancer Therapy. *Nat. Nanotechnol.* **2007**, *2*, 751–760.
- Zhang, L.; Gu, F. X.; Chan, J. M.; Wang, A. Z.; Langer, R. S.; Farokhzad, O. C. Nanoparticles in Medicine: Therapeutic Applications and Developments. *Clin. Pharmacol. Ther.* **2008**, *83*, 761–769.
- Mornet, S.; Vasseur, S.; Grasset, F.; Duguet, E. Magnetic Nanoparticle Design for Medical Diagnosis and Therapy. *J. Mater. Chem.* **2004**, *14*, 2161–2175.
- Corot, C.; Robert, P.; Idee, J. M.; Port, M. Recent Advances in Iron Oxide Nanocrystal Technology for Medical Imaging. *Adv. Drug Delivery Rev.* **2006**, *58*, 1471–1504.
- Mebius, R. E.; Kraal, G. Structure and Function of the Spleen. *Nat. Rev. Immunol.* **2005**, *5*, 606–616.
- Perrault, S. D.; Walkey, C.; Jennings, T.; Fischer, H. C.; Chan, W. C. W. Mediating Tumor Targeting Efficiency of Nanoparticles through Design. *Nano Lett.* **2009**, *9*, 1909–1915.
- Moghimi, S. M.; Porter, C. J.; Muir, I. S.; Illum, L.; Davis, S. S. Non-phagocytic Uptake of Intravenously Injected Microspheres in Rat Spleen: Influence of Particle Size and Hydrophilic Coating. *Biochem. Biophys. Res. Commun.* **1991**, *177*, 861–866.
- Zhang, G. D.; Yang, Z.; Lu, W.; Zhang, R.; Huang, Q.; Tian, M.; Li, L.; Liang, D.; Li, C. Influence of Anchoring Ligands and Particle Size on the Colloidal Stability and *In Vivo* Biodistribution of Polyethylene Glycol-Coated Gold Nanoparticles in Tumor-Xenografted Mice. *Biomaterials* **2009**, *30*, 1928–1936.
- Choi, H. S.; Liu, W.; Misra, P.; Tanaka, E.; Zimmer, J. P.; Ipe, B. I.; Bawendi, M. G.; Frangioni, J. V. Renal Clearance of Quantum Dots. *Nat. Biotechnol.* **2007**, *25*, 1165–1170.
- Geng, Y.; Dalhaimer, P.; Cai, S. S.; Tsai, R.; Tewari, M.; Minko, T.; Discher, D. E. Shape Effects of Filaments *versus* Spherical Particles in Flow and Drug Delivery. *Nat. Nanotechnol.* **2007**, *2*, 249–255.
- Park, J. H.; von Maltzahn, G.; Zhang, L. L.; Derfus, A. M.; Simberg, D.; Harris, T. J.; Ruoslahti, E.; Bhatia, S. N.; Sailor, M. J. Systematic Surface Engineering of Magnetic Nanoworms for *In Vivo* Tumor Targeting. *Small* **2009**, *5*, 694–700.
- Merkel, T. J.; Jones, S. W.; Herlihy, K. P.; Kersey, F. R.; Shields, A. R.; Napier, M.; Luft, J. C.; Wu, H.; Zamboni, W. C.; Wang, A. Z.; *et al.* Using Mechanobiological Mimicry of Red Blood Cells To Extend Circulation Times of Hydrogel Microparticles. *Proc. Natl. Acad. Sci. U.S.A.* **2011**, *108*, 586–591.
- Mitragotri, S.; Lahann, J. Physical Approaches to Biomaterial Design. *Nat. Mater.* **2009**, *8*, 15–23.
- Jiang, S. Y.; Cao, Z. Q. Ultralow-Fouling, Functionalizable, and Hydrolyzable Zwitterionic Materials and Their Derivatives for Biological Applications. *Adv. Mater.* **2010**, *22*, 920–932.
- Yang, W.; Zhang, L.; Wang, S. L.; White, A. D.; Jiang, S. Y. Functionalizable and Ultra Stable Nanoparticles Coated with Zwitterionic Poly(carboxybetaine) in Undiluted Blood Serum. *Biomaterials* **2009**, *30*, 5617–5621.
- Zhang, L.; Xue, H.; Gao, C. L.; Carr, L.; Wang, J. N.; Chu, B. C.; Jiang, S. Y. Imaging and Cell Targeting Characteristics of Magnetic Nanoparticles Modified by a Functionalizable Zwitterionic Polymer with Adhesive 3,4-Dihydroxyphenyl-L-Alanine Linkages. *Biomaterials* **2010**, *31*, 6582–6588.

21. Carr, L. R.; Zhou, Y. B.; Krause, J. E.; Xue, H.; Jiang, S. Y. Uniform Zwitterionic Polymer Hydrogels with a Nonfouling and Functionalizable Crosslinker Using Photopolymerization. *Biomaterials* **2011**, *32*, 6893–6899.
22. Zhang, L.; Xue, H.; Cao, Z.; Keefe, A.; Wang, J.; Jiang, S. Multifunctional and Degradable Zwitterionic Nanogels for Targeted Delivery, Enhanced MR Imaging, Reduction-Sensitive Drug Release, and Renal Clearance. *Biomaterials* **2011**, *32*, 4604–4608.
23. Cai, Q.; Kim, S. H.; Choi, K. S.; Kim, S. Y.; Byun, S. J.; Kim, K. W.; Park, S. H.; Juhng, S. K.; Yoon, K. Colloidal Gold Nanoparticles as a Blood-Pool Contrast Agent for X-ray Computed Tomography in Mice. *Invest. Radiol.* **2007**, *42*, 797–806.
24. Kim, D.; Park, S.; Lee, J. H.; Jeong, Y. Y.; Jon, S. Antibiofouling Polymer-Coated Gold Nanoparticles as a Contrast Agent for *In Vivo* X-ray Computed Tomography Imaging. *J. Am. Chem. Soc.* **2007**, *129*, 7661–7665.
25. Cheng, J. J.; Teply, B. A.; Sherifi, I.; Sung, J.; Luther, G.; Gu, F. X.; Levy-Nissenbaum, E.; Radovic-Moreno, A. F.; Langer, R.; *et al.* Formulation of Functionalized PLGA-PEG Nanoparticles for *In Vivo* Targeted Drug Delivery. *Biomaterials* **2007**, *28*, 869–876.
26. Mohanraj, V. J.; Chen, Y. Nanoparticles—A Review. *Trop. J. Pharm. Res.* **2006**, *5*, 561–573.
27. Redhead, H. M.; Davis, S. S.; Illum, L. Drug Delivery in Poly(lactide-co-glycolide) Nanoparticles Surface Modified with Poloxamer 407 and Poloxamine 908: *In Vitro* Characterisation and *In Vivo* Evaluation. *J. Controlled Release* **2001**, *70*, 353–363.